Engineering Science and Military Technologies
Volume (8) - Issue (2) - Sep 2024
ISSN: 2357- 0954
DOI:10.21608/EJMTC.2024.245238.1273

Finite element analysis of a single point incremental forming of foot supports

Original Article

Abdelrahman A. A. Abouzeid[1], Ahmed M. Elkassas[1], Mohsen A Hassan[2], Nader N. Zaafarani[1]

[1]Department of Production Engineering and Mechanical Design, Tanta University Tanta, [2]Materials Science and Engineering Program, Egypt Japan University of Science and Technology, Egypt

Keywords:
Formability, Foot supports, FEA, Incremental sheet forming

Corresponding Author:
Abdelrahman A. A. Abouzeid, Department of Production Engineering and Mechanical Design, Tanta University, Tanta, Egypt, **Tel.:** 01157467452, **Email:** abdelrahmanabuzaid1993@gmail.com

Abstract
In this study, the incremental sheet-forming (ISF) process of foot supports was simulated using finite-element analysis (FEA). The study employed ABAQUS/Explicit finite-element software to study the characteristics of manufacturing such complicated shapes. Several simulation runs have been conducted to ensure the feasibility of the ISF approaches proposed in this work, whereas the numerical results have been confirmed by experimental tests. An error analysis of the thickness distribution was made to compare the theoretical, measured, and simulation results. The results revealed that themaximum thinning occurred at the wall of the foot support product. The comparison showed that the variation in simulated and experimental depth along the profile of the product base didn't exceed 8%. Furthermore, the vertical reaction force on the forming tool increases with forming depth until a specific maximum value and remains approximately constant until the onset of sheet cracking, then starts to decrease. Also, strain increased gradually and reached its maximum value at a depth of 25 mm. Energy consumption in deep drawing shows a reduction of 2.5 times that consumed in the ISF process for the same final depth.

1. INTRODUCTION

Incremental sheet forming (ISF) refers to a sequence of localized deformations that are presented during various forming processes. The appropriate shape is achieved by carrying out these deformations progressively along a predetermined path, enabling the material to deform to extraordinarily high levels, producing a wide range of forms without the use of expensive or specialized equipment[1-3]. Incremental sheet forming is becoming more important due to its many industrial applications in the production process, such as electronics, aircraft[3], automobiles[4], medicinal devices[5], and a variety of other items. ISF generally approaches spinning; however, there are several significant variances[6]. An analytical model, proved by experimental observations on the aluminum alloy sheets of designations 1100, 2024, 5052, and 6111, was developed to assess the stress state, the frictional influence on Single Point Incremental Forming (SPIF), and build a connection between the stress state and forming parameters to get a thorough understanding of the ISF process[7]. Recent research has brought incremental forming numerical simulation to the attention of certain scholars to understand the variables impacting the SPIF process and their effect on the forming of steel sheets. Pepelnjak *et al.*[8] contrasted a finite element (FE) analysis of a pyramid that was constructed progressively with experimental validation on ISF processing of DC04 low-carbon steel. The accuracy of the simulated developed shape, particularly in relation to the part's geometric precision and the bottom pillowing effect, was impacted by growing the element size. The highest geometrical accuracy was discovered at a mesh size of 1×1 mm, with a mass scaling of 19.01 and a tool velocity of 16.49 m/s. Oliaei *et al.*[9] studied the effects of particular process variables on residual stresses and the distributions of component thickness during incremental sheet metal forming of the aluminum alloy 1100. According to a comparison study between FEA and experiments, the maximum difference in thickness between forecasts and evaluation does not exceed 8%. Additionally, it has been demonstrated that bigger tools produce forms with greater depth and force. Step overs improve formability and lower forming-induced stresses. He *et al.*[10] studied the influence of forming strategy on the opening or closing of rings taken from a truncated cone manufactured by SPIF. The

results show that the forming strategy should be carefully chosen to minimize the opening or closing of the rings and improve the accuracy of the final product.Salem *et al.*[11] examined how the tool path affects the thickness variation during single point incremental forming (SPIF) of a7075-O aluminum alloy sheet. The SPIF process is simulated using a finite element model, and the results are contrasted with experimental analyses. According to the results, the tool path significantly affects the thickness variation, with the bending area exhibiting the most severe thinning. Additionally, it has been observed that the tool's initial contact with the sheet resulted in the highest thinning. An analytical model has been investigated by Zhu *et al.*[12] to predict forming force during the ISF process fora truncated cone, pyramid part, and cranial plate,considering the impact of global bending, contact conditions, and material deformation. And so did Singh *et al.*[13], but more than that, the results of the model have been compared with simulation and numerical results, recording a 4.89% maximum error percentage. Saad *et al.*[14] presented the application of ISF in dentistry to manufacture a stainless steel denture plate, noting the satisfactory dimensional accuracy of the manufactured components. Benmessaoud[15] developed a FEM of the SPIF process of AA3003-H12 sheets to clarify the mechanisms of fracture and failure in the manufactured part. It has been noted that the critical regions were found at the corner of the part.

In earlier works, researchers have concentrated on simple geometries like the cone and pyramid. Complicated prefabricated products, such as foot support, need to be customized according to the foot shape and size of the patient. Therefore, they are produced according to a computed tomography scan of the patient.Nevertheless, as the produced foot supports need to be in perfect fit, the determination of the effect of the production method on the product shape accuracy is immense. Therefore, a simulation of the manufacturing processes of the foot supporthelpsin predicting the accuracy of the process and hence the suitability of utilizing this specific manufacturing technique.However, there are very few published studies on the numerical modelling and experimental verification of foot support manufacturing[16,17]. The goal of this research is to combine numerical modelling and experimental verification to investigate the effects of process parameters on the product of incrementally manufactured metal foot supports. In this study, thickness distribution, profile accuracy, reaction force, and consumed energy have been demonstrated. This paper has the following structure: section 1 outlines methodology used in the current investigation, and section 2 shows the obtainable results that can be reached, and a discussion of the association between simulation results correspond with those of the experiments. Eventually, the last section summarizes the main findings, the implications of the results, and the limitations of the study.

1. Methodology

1.1. Experimental Work

According to JIS G3131-2005 standards[18], a steel sheet with a 1.1 mm initial thickness and the grade SPHC was selected as the deformed material for this work. The chemical composition of the sheet supplied by the Egyptian company AL EZZ DEKHEILA STEEL COMPANY (S.A.E.) is shown in Table 1. All investigations utilized steel sheets with blank sizes of (400 mm × 250 mm).

Table 1: Chemical Composition of the steel sheets

Element	C	Si	Mn	P	S	Al	N
Wt %	0.05	0.02	0.24	0.006	0.003	0.040	0.056

To characterize the used material, tension tests are performed on samples that were laser cut from the material sheet metal in three different orientations with respect to (θ) the sheet rolling direction in accordance with ISO 6892-1[19], as shown in Figure 1. A SHIMADZU Universal Testing Machine, model AG100KNXplus, was used to conduct uniaxial tensile testing with a constant strain rate of 0.0011/sec.

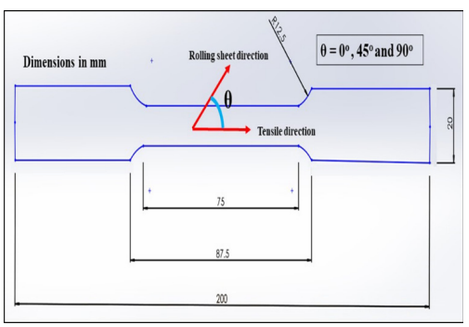

Fig. 1: The tensile test specimen dimensions according to (ISO 6892-1)

Figure 2 illustrates the true stress-truestrain curve of the examined material by distinct curvature for three directions, involving the rolling direction, perpendicular to the rolling direction, and the 45° direction.

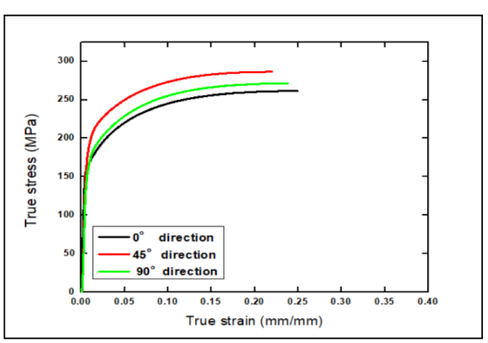

Fig. 2: True stress - strain curve for SPHC steel specimens

To carry out the ISF process and afterwards evaluate the desired geometry of the foot support, experimental tests were completed on the threeaxes Fadal 88H milling machine illustrated in Figure 3.

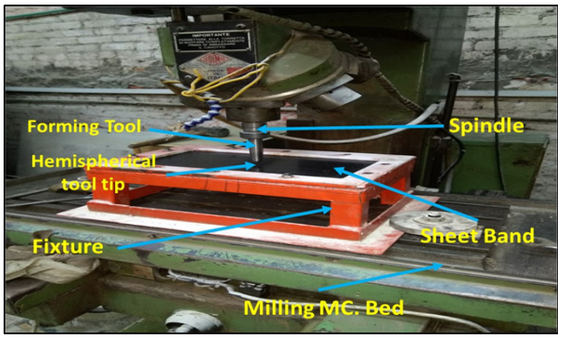

Fig. 3: Photo for the setup used in SPIF and the fixation of forming tool in CNC machine

The route of the tool starts from the outer periphery of the product and travels along the whole contour. After that, it was fed horizontally inwards the product and downwards the vertical direction, according to the data listed in Table 2. A tool with a hemi-spherical tip of 16 mm diameter was utilized. The tool is built of tool steel supplied by Böhler Company of type K100, which has undergone heat treatment to improve the hardness to 65 HRC, enhancing wear resistance and preventing any change in tool profile. The foot support profile was selected as the toolpath. POWERMILL CAM software was used to produce a toolpath file for the single-pinforming tool. Figure 4 is an isometric view of theISF of foot support dimensions, whereas Table 2 lists the fixed parameters in the ISF process.

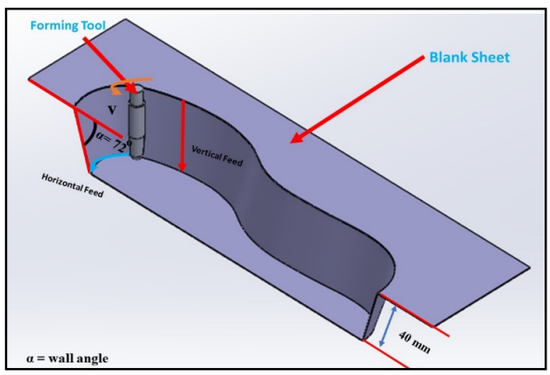

Fig. 4: Isometric view of ISF of foot support and dimensions

1.2. Finite Element Analysis

1.2.1. Model generation

During the ISF process, high non-linearity and significant plastic deformation must be taken into consideration in the simulation, including localized plastic deformation. In the current study, the explicit dynamic FEA setup on the commercial program ABAQUS was used to simulate the ISF process under consideration.

• Creating the geometry Solid models

The explicit dynamic model that has been developed consists of two parts: the sheet from which the shape is to be developed and the tool used in forming the sheet. The type of sheet is selected as a 3D deformable, planar shell with a rectangular shape with dimensions (400 mm × 250 mm) assuming a homogeneous shell formulation. The Tool is selected as a 3D discrete rigid. The forming tool was modelled as a rigid body with a hemispherical end, and during the simulation, a node was selected as a reference node (RP), and the force values were measured at this node.

•Mesh

Figure 5 shows a full view of a simple setup for the implementation of simulations and experimentsclose to the tool matching the blank. A specific shell thickness will be used to mesh the sheet with shell elements. To simulate the ISF process, a dynamic explicit FE code is used. It uses full explicit time integration to address precisely dynamic problems with elastic-plastic isotropic material model, with data from the tension test. Since the mesh size has an important influence on the simulation results, its effect was examined. Two elements with sizes of 10× 10 mm2 and 5 × 5 mm2 were selected. The results deviation is approximately 14%.To adjust the cell size before meshing the part, the edges must first be seeded. Next, the mesh controls must be set, in which the element type is specified to be shell elements, linear quadrilateral elements of Type 4 integration points (S4R).The process time for 10 mm element size was 25 min, whereas it was 70 min for 5 mm element size. However, the increasein FE size reduced the computation time but increased the geometrical error. However, the simulation process can also run faster throughout reducing the output request to satisfy needed output or using more cores of the laptop processor.

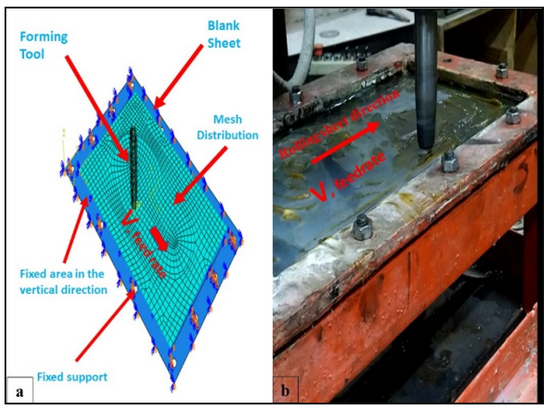

Fig. 5: ISF representation, (a) Simulation and (b) Experimental

Table 2: Fixed ISF parameters.

Input Parameter	Value	Unit
Blank thickness	1.1	mm
Wall angle	72º	deg
Product deep depth	40	mm
Tool size	16	mm
Vertical step size	0.8	mm
Feedrate	300	mm/min
Spindle speed	500	rpm
Tool type	spherical tip	
Lubricant	grease	
Tool path	step wise	

1.2.2. Material models

Besides the ISF parameters listed in Table 2, other physical and mechanical characteristics of the hot-rolled steel sheet metal are summarized in Table 3. The hardening characteristics of the sheet material were modelled using the isotropic strain hardening rule, which is given by the exponential equation

$$\sigma = K \varepsilon^{n}$$

Where K is the strength coefficient of thematerial and n is the strain hardening coefficient extracted from the tensile tests performed on the sheet materials.

Table 3: Material properties

Input Parameter	Value	Unit
Young's modulus	200	GPa
Average yield stress (sY)	150	MPa
Average ultimate tensile strength	276	MPa
Average strain hardening coefficient (K)	337	MPa
Poisson's ratio	0.27	
Average strain hardening exponent (n)	0.225	
Density of sheet metal	7800	kg/m3

1.2.3. Boundary and Contact Conditions

To model the bolt's fixation and the fixture's fastening effect, an Encastre boundary condition was applied to the exterior region of the sheet metalwhich extends 30 mm from the sheet edge along the sheet perimeter. The tool route of motion for each experiment was generated by G-codes extracted from Powermill CAM software. Noting that it starts, as in the experiment, from the outer periphery and then towards the inside before feeding. The interaction between the tool and the sheet was referred to as surface-to-surface contact, whereasthe tool was defined as themaster surface and thesheet was defined as the slave surface.The Coulomb coefficient of friction of the lubricant used in the process was taken to be 0.06[20].

To compare the ISF process with the conventional forming technique, a Finite Element Simulation of deep drawing (DD) process of the investigated foot support has been carried out with the boundary and contact conditions, as shown in Figure 6. A surface-to-surface dynamic explicit contact with afinite "sliding penalty" based contact technique was utilized in conjunction with three contact pairs: punch-top blank (μp =0.15), holder-top blank (μh = 0.1), and die-bottom blank (μd =0.1) to effectively represent the interaction of rigid and deformable components [21]. The punch draws the sheet to 30 mm depth with apunch speed of 0.1 mm/sec.

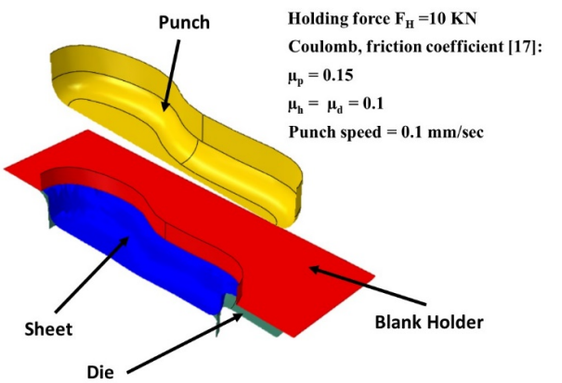

Fig. 6: Representation of boundary and contact condition in deep drawing

2. Results and Discussion

2.1. Thickness Distribution

The tool movement in the simulation successively affected the thickness of the product in the bending zone, which starts near the clamped surface of the product. While the product depth with ISF had reached 25 mm before cracking (i.e., thefailure criterion is achieved by exceeding the forming limit of the material), the DD process revealed a successful 30 mm forming depth.The process, either through experimentation or simulation was ended at the onset of fracture, at which the extreme values were reached. Then the values start to return to their original values.

Figures 7 and 8illustrate the development of the reduction in sheet thickness along the defined path and the equivalent strain during the ISF and deep drawing (DD) processes at different positions on the path P1-P4 shown. Position 1 (P1), which is near the blank edge, is the first to involve deformation throughout the simulation. It may be noticed that small strains were implicated in the ISFprocess untilend of formingbecause it only affected by the tool action for few contours. Also, there is no remarkable decrease in thickness along the selected path up to 12 mm depth as a geometry irregularity occurs at a position between points P1 and P2 (Figure 7).

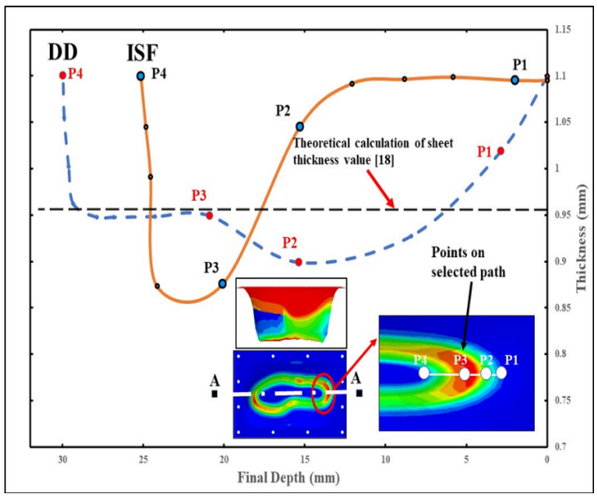

Fig. 7: Change of sheet thickness at cross section A-A up to maximum reached depth

At position P3 at the corner of the product, stresses concentrate, leading to a rapid decrease in thickness up to 25 mm depth. At this depth, the minimum thickness reaches 0.873 mm near position P3, which is about 8% smaller than the theoretically calculated thickness reduction value based on the sine law (t1 = t0cos (90º − α) = t0sin (α)[22] and represents the largest thickness reduction. The error function for the difference inthickness obtained analytically was defined as:

$$Percentage\ error = [\frac{t_{theor} - t_{measured}}{t_{theor}}] \times 100$$

Maximum strains are accompanied by the maximum stretching in the sheet (near P3) inthe ISF process. The strains decline gradually until they almost vanish at P4 near the bottom base and at P1 near the sheet fixation.Compared to DD, a more gradual reduction in sheet thickness is observed at a position between P1 and P2, as the whole sheet is subjected once to geometry irregularity. After the sheet proceeds with this irregularity, it is subjected to straining in the product wall. Equivalent strain has a uniform pattern for all positions up to a depth of 20 mm and then increases gradually until fracture reaches the maximum value at P3.This increase in strain isdue to the high stretch on the product wall at this position and hence thinning in the sheet thickness (see Figure 7). Then, it decreases at position P4, as the sheet breaks free from the blank holder force slides intothe die. This shows the non-uniformityof the drawing in the ISF process counter to DD, at which a noticeable uniform strain distributionoccurs because of thesliding of the sheet in the DD process, whereas it is clamped in the ISF.In order to evaluate the strain at certain locations after forming experimentally, grid marking is applied. After the forming process, the deformed ellipse was measured to estimate the strain values at fracture. A single-circle grid type was used in this work; it was performed using the manual approach. A circular mold pattern with an 8-mmdiameter and a spray were used to print the grids on the surface of the steel sheet. The measurement of the circles and the produced ellipses was carried out using a simple flexible curve ruler.

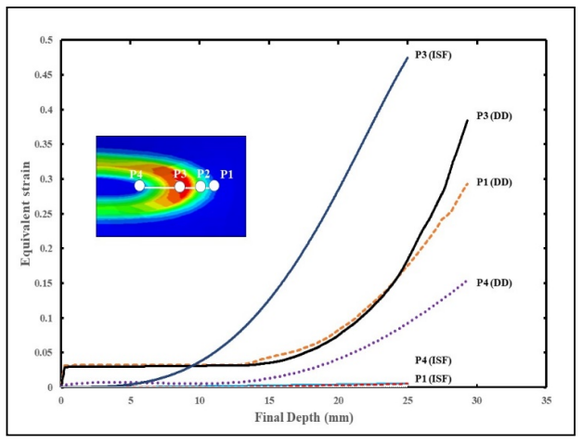

Fig. 8: Strain development during the ISF and DD processes at selected positions

2.2. Geometrical accuracy

Geometrical accuracy considers the shape of the finished product by comparing the original profile taken from the CAD work with the simulated profile provided by FE simulations and experimental work, as shown in Figure 9. It can be observed that the maximum error didn't exceed 8% of the point depth between the simulated and experimental profiles of the product base. These deviations resulted from the effect of the springback,the tool radius effect at the corner of the product, and the material's pillow effect at the bottom of the product.

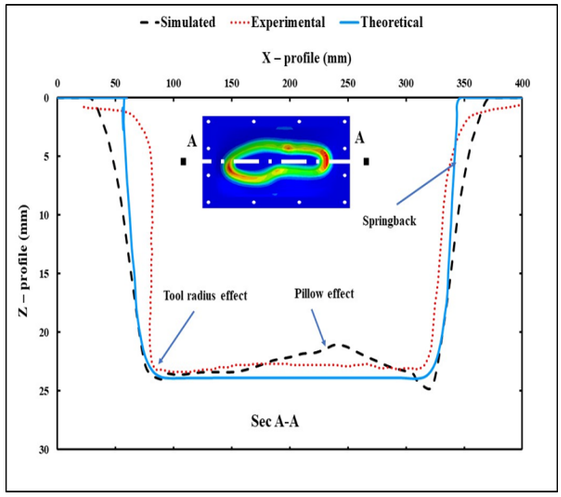

Fig. 9: Comparison between numerical, theoretical and experimental profile

Figure 10 displays height contours from FEA, plotted on the cross-section of the deformed product. Regions A–Brepresent the tool and the sheet contact, and regions F1–F2 describe the fixture clamps of the sheet. The regions of the sheet between the fixture clamp sections performed as a simply supported beam, and the forming force on the tool performed as a concentrated load at the tool-sheet contact. Thus, the induced bending moment yields the sheet to be formed.

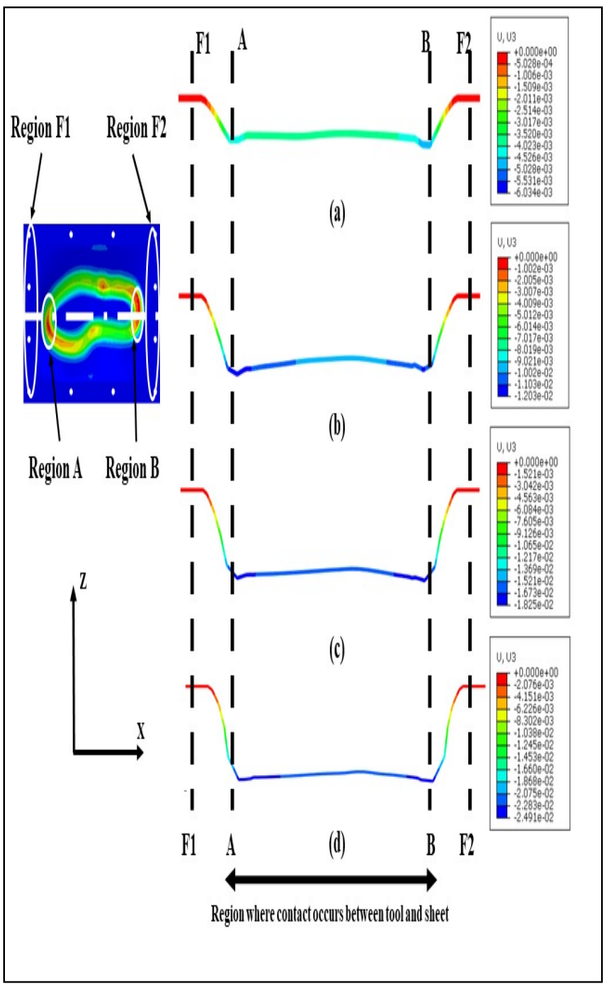

Fig. 10: Contours of Z displacement from FEA at forming heights of (a) 6 mm (b) 12 mm, (c) 18 mm, and (d) 25 mm

2.3. Reaction forces and consumed energy

The force needed for forming has an impact on the design of fixtures and tooling. As was already indicated, the equipment used for the current study was a standard CNC milling machine not specifically assigned to forming operations. To prevent any possible damage to the machine, it was essential to calculate the forces exerted on the machine's axis throughout the forming process.

Figure 11 compares the development of the exerted vertical forming force during the ISF and DD processes of the investigated sheet.As seen in Figure 11-a, the force increases during the first contours to reach a maximum value at a depth of 25 mm as the tool pushes further against the blank until it eventually reaches a depth where the forces tend to remain approximately constant. Also, as expected, the vertically exerted reaction force on the machine axis is greater than the resultant horizontal force. Comparing forces in ISF and DD shows that the force required for DD is about two orders of magnitude larger than these in ISF.

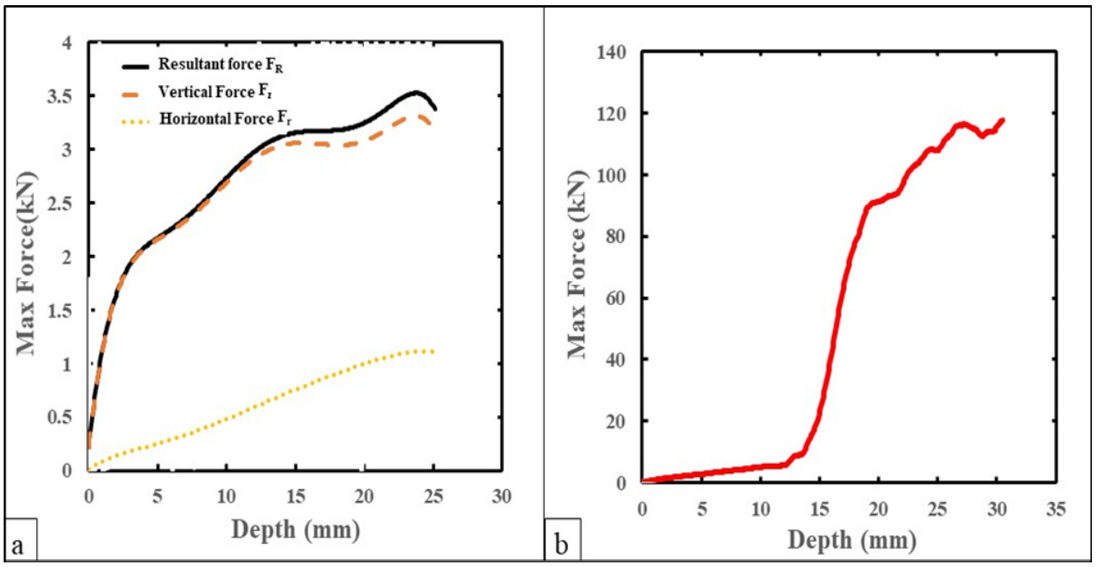

Fig.11: Development of forming force, (a) Forces in ISF process, and (b) Vertical force in DD

As shown in Figure 11-a, the vertical force increases rapidly at the initial contours due to the transverse layout of the sheet with respect to the tool direction. As the sheet deforms, the rate of increasing the vertical force slows down up to the end of deformation. On the other hand, drawing force in DD begins slightly small as the sheet slides with the punch movement as illustrated in Figure 11-b, but due to the irregular shape of the product, local strains have been developed, as discussed earlier, in specific regions. This results in high strain hardening of the material, and starting from a forming depth of 15 mm, the drawing force increases at a rapid rate with further increases in product final depth.

The comparison illustrated in Figure 12 shows that the total energy consumed in the ISF process to reach a depth of 25 mm is about 2.5 times that of the DD process for the same depth. Besides the need to overcome the continuous friction applied to the forming tip in ISF process, another factor justifies the higher energy consumption in ISF. The ISF process can be treated as a continuous loading-unloading process, as when the forming tool leaves the local forming area, the material rebounds elastically till the nest contour, where the forming tool acts at the vertical step size from that relaxed position apart. The forming tool needs to first overcome the elasticity in the material, as if the deformation starts from the beginning before ant plastic deformation takes place. Taking into account that energy consumed in simulation is strain energy.

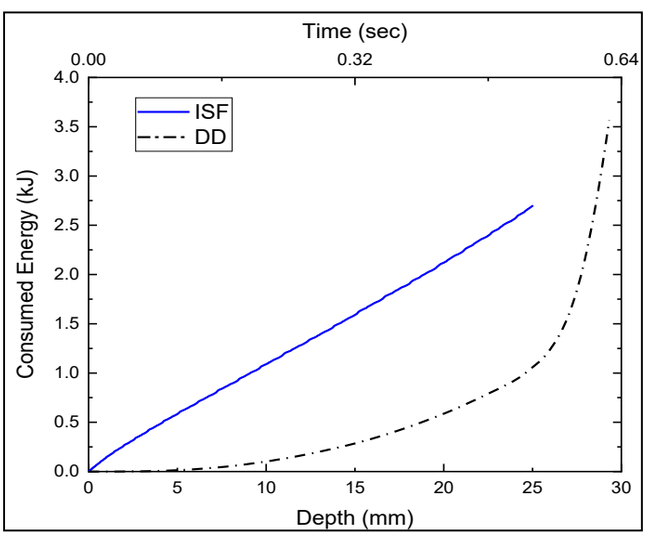

Fig. 12 : Energy consumption in ISF and DD processes

3. Conclusion

This study simulates a single point incremental forming process by developing a finite element model with an isotropic hardening material behavior. The results display that major deformations have been situated along the contour of foot support, but it must be noted that:

• There are slight deformations on the borders near the clamped shape. The critical regions can be found at a small curvature radius at the lower place of the product wall, so special care must be taken during deformation with ISF, especially at corners, as the simulation results show significant thickness reduction.

• There are small deviations betweenthe theoretical,simulation, and experimental product final profile resulting from the effect of the springback, tool radius effect at the corner of the product, and the material's pillow effect at the bottom of the product.

• In the case of using ISF as a small batch production method instead of DD, a feasibility study needs to be performed considering the energy consumption in each process.

4. References

[1] U. Khalil, H. Aziz, M. Jahanzaib, W. Ahmad, S. Hussain, and F. Hafeez, "Effects of Forming Tools and Process Parameters on Surface Roughness in Incremental Sheet Forming, a Review," Adv. Sci. Technol. Res. J., vol. 12, no. 3, pp. 75–95, 2018, doi: 10.1291390223/22998624/.

[2] C. Bouffioux, C. Henrard, J. Gu, J. R. Duflou, A.-M. Habraken, and H. Sol, "Development of an Inverse Method for Identification of Materials Parameters in the Single Point Incremental Forming Process," in International Deep-drawing Research Group IDDRG 2007 International Conference 2123- May 2007, Győr-Hungary Proceedings ed. by M. Tisza, 2007.

[3] A. Barimani-Varandi, M. K. Nasrabadi, B. A. Ravan, and M. Javadi, "Rapid Prototyping of Aircraft Canopy Based on the Incremental Forming Process," J. Brazilian Soc. Mech. Sci. Eng., vol. 43, no. 2, pp. 1–15, 2021, doi: 10.1007/s404301-02811-021-.

[4] J. Li, J. Shen, and B. Wang, "A Multipass Incremental Sheet Forming Strategy of a Car Taillight Bracket," Int. J. Adv. Manuf. Technol., vol. 69, no. 9–12, pp. 2229–2236, 2013, doi: 10.1007/s001703-5179-013-.

[5] S. Gatea and H. Ou, "Surface Roughness Analysis of Medical Grade Titanium Sheets Formed by Single Point Incremental Forming," Int. J. Adv. Manuf. Technol., vol. 114, no. 9–10, pp. 2975–2990, 2021, doi: 10.1007/s001709-07056-021-.

[6] G. Hussain, H. R. Khan, L. Gao, and N. Hayat, "Guidelines for Tool-Size Selection for Single-Point Incremental Forming of an Aerospace Alloy," Mater. Manuf. Process., vol. 28, no. 3, pp. 324–329, 2013, doi: 10.108010426914.2012.700151/.

[7] B. Lu *et al.*, "Mechanism Investigation of Friction-Related Effects in Single Point Incremental Forming Using a Developed Oblique Roller-Ball Tool," Int. J. Mach. Tools Manuf., vol. 85, pp. 14–29, 2014, doi: 10.1016/j.ijmachtools.2014.04.007.

[8] T. Pepelnjak, L. Sevšek, O. Lužanin, and M. Milutinović, "Finite Element Simplifications and Simulation Reliability in Single Point Incremental Forming," J. Mater., vol. 15, no. 10, pp. 1–22, 2022, doi: 10.3390/ma15103707.

[9] S. N. B. Oliaei, M. Eivazzadeh, and S. Dadvandipour, "Finite Element Modeling of Incremental Sheet Metal Forming of Aluminum Alloy Al 1100," in Scientific Proceedings XIV International Congress "Machines. Technologies. Materials, 2017, vol. 4, pp. 254–257.

[10] S. He *et al.*, "Finite Element Modeling of Incremental Forming of Aluminum Sheets," Adv. Mater. Res., vol. 6–8, pp. 525–532, 2005, doi: 10.4028/www.scientific.net/amr.68.525-.

[11] E. Salem, J. Shin, M. Nath, M. Banu, and A. I. Taub, "Investigation of Thickness Variation in Single Point Incremental Forming," Procedia Manuf., vol. 5, pp. 828–837, 2016, doi: 10.1016/j.promfg.2016.08.068.

[12] H. Zhu and H. Ou, "A New Analytical Model for Force Prediction in Incremental Sheet Forming," J. Mater. Process. Tech., vol. 318, pp. 118–137, 2023, doi: 10.1016/j.jmatprotec.2023.118037.

[13] R. P. Singh, S. Kumar, P. K. Singh, and A. K. Srivastwa, "A Mathematical Model for Force Prediction in Single Point Incremental Sheet Forming with Validation by Experiments and Simulation," Processes, vol. 11, pp. 1688–1711, 2023, doi: 10.3390/pr11061688.

[14] S. S. A. A. Hassan Saad, Ahmed Z. M. Shammari, "Fabrication and Analysis of Denture Plate Using Single Point Incremental Sheet Forming," Al-Khwarizmi Eng. J., vol. 19, no. 2, pp. 68–81, 2023, doi: 10.22153/kej.2023.02.001.

[15] R. Benmessaoud, "Incremental Sheet Forming Process of an AA3003-H12 Part: Simulation Study and Experimental Validation," Int. J. Comput. Mater. Sci. Eng., vol. 12, no. 4, 2023, doi: 10.1142/S2047684123500112.

[16] G. Ambrogio, L. De Napoli, L. Filice, F. Gagliardi, and M. Muzzupappa, "Application of Incremental Forming Process for High Customised Medical Product Manufacturing," J. Mater. Process. Technol., vol. 162–163, pp. 156–162, 2005, doi: 10.1016/j.jmatprotec.2005.02.148.

[17] V. Gulati, S. Kathuria, and P. Katyal, "A Paradigm to Produce Customized Ankle Support Using Incremental Sheet Forming," J. Eng. Technol., vol. 5, no. 1, p. 14, 2015, doi: 10.41038580.149474-0976/.

[18] JIS 2005, "Global Marketing for Tube & Pipe," Available 20 September 2016, at <https://www.scribd.com/document/324684522/JIS-G3131>.

[19] ISO 68922019 1-, "Metallic materials — Tensile testing — Part 1: Method of test at room temperature," Available 4 December2019, at <https://www.iso.org/obp/ui/es/#iso:std:iso:6892:-1:ed-3:v1:en>.

[20] U. A. Deta, N. Suprapto, H. Mubarok, A. S. Adam, and A. Kholiq, "The Comparison of Static Friction Coefficient on Wood Between the Combination of Wood-Metal Load System and Wood-Sand Load System," in International Conference on Science and Technology (ICST), 2018, vol. 1, pp. 887–890. doi: 10.2991/icst-18.2018.179.

[21] M. J. Jweeg, A. I. Mohammed, and M. S. Jabbar, "Investigation of Thickness Distribution Variation in Deep Drawing of Conical Steel Products," Eng. Technol. J., vol. 39, no. 04, pp. 586–598, 2021, doi: 10.30684/etj.v39i4A.1908.

[22] G. Hussain, L. Gao, and N. U. Dar, "An Experimental Study on Some Formability Evaluation Methods in Negative Incremental Forming," J. Mater. Process. Technol., vol. 186, no. 1–3, pp. 45–53, 2007, doi: 10.1016/j.jmatprotec.2006.12.005.